

# Differentially-rotating neutron star models with a parametrized rotation profile

Filippo Galeazzi<sup>1\*</sup>, Shin'ichirou Yoshida<sup>2</sup>, Yoshiharu Eriguchi<sup>2</sup>

<sup>1</sup> Max-Planck-Institut für Gravitationsphysik, Albert-Einstein-Institut, Am Mühlenberg 1, D-14476 Potsdam, Deutschland

<sup>2</sup> Department of Earth Science and Astronomy, Graduate School of Arts and Sciences, University of Tokyo, Komaba, Meguro-ku 3-8-1, 153-8902 Tokyo, Japan

Received / Accepted

## ABSTRACT

We analyze the impact of the choice rotation law on equilibrium sequences of relativistic differentially-rotating neutron stars in axisymmetry. The maximum allowed mass for each model is strongly affected by the distribution of angular velocity along the radial direction and by the consequent degree of differential rotation. In order to study the wide parameter space implied by the choice of rotation law, we introduce a functional form that generalizes the so called “j-const. law” adopted in all previous work. Using this new rotation law we reproduce the angular velocity profile of differentially-rotating remnants from the coalescence of binary neutron stars in various 3-dimensional dynamical simulations. We compute equilibrium sequences of differentially rotating stars with a polytropic equation of state starting from the spherically symmetric static case. By analyzing the sequences at constant ratio,  $T/|W|$ , of rotational kinetic energy to gravitational binding energy, we find that the parameters that best describe the binary neutron star remnants cannot produce equilibrium configurations with values of  $T/|W|$  that exceed 0.14, the criterion for the onset of the *secular* instability.

**Key words.** relativity – gravitation – stars: rotation – stars: interiors – stars: neutron

## 1. Introduction

A neutron star (NS), during most of its life, is considered to be a stationary and rigidly rotating object, apart from a tiny lag between the rotation of the superfluid component and that of the normal fluid and the crust (e.g. Baym et al. (1969) and Pines & Alpar (1985)).

In fact a nascent neutron star which is born in a supernova event is likely to rotate differentially at first before its angular velocity distribution evolves toward a uniform rotation. There are several mechanisms that account for the redistribution of the angular momentum. One such mechanism is the shear viscosity of neutron matter (Sawyer 1989). An estimate of the timescale in which the viscosity damps a neutron star’s internal shear motion has received a lot of attention in the literature (e.g. Cutler & Lindblom (1987)). For a typical neutron star we expect a timescale of 10 – 100 yrs. In the presence of magnetic fields, the magnetic braking (Spruit 1999) or the magnetorotational instability (MRI) (Balbus & Hawley 1991) may drastically accelerate the redistribution of angular momentum to the order of 1s (Duez et al. 2006).

Differential rotation plays an important role in the beginning and at the end of the life of a NS. In its early life, strong differential rotation of a massive core in a supernova may affect the collapse and bounce dynamics (Dimmelmeier et al. 2002; Ott et al. 2004). A newly-born neutron star with strong differential rotation may lose its stability in the course of the rotational (and thermal) evolution, and may collapse to a black hole or other type of compact star (quark star, hybrid star). This may give a unique neutrino signal and a strong gravitational wave emission from the supernova explosion of massive stars (see, e.g.,

Ott et al. (2007) and Takiwaki & Kotake (2010) for recent studies on gravitational wave mechanism from stellar core collapse).

An exciting way in which a neutron star’s life can end is in the inspiral and consequent merger with a binary companion. Recent results of numerical 3-dimensional simulations of neutron star binary mergers (e.g., Ruffert et al. (1996); Ruffert & Janka (2001); Shibata & Uryū (2002); Shibata & Taniguchi (2006); Anderson et al. (2008); Baiotti et al. (2008); Giacomazzo et al. (2010)) have shown that there are cases in which the remnant of the merger has a significantly high degree of differential rotation such that it can sustain a total mass considerably larger than that of a uniformly rotating star (Baiotti et al. 2008). These hyper-massive neutron stars (HMNSs) remain stable over many dynamical timescales before collapsing to a BH (e.g. Shibata & Uryū (2002), Baiotti et al. (2008)). In order to study the effect of the centrifugal force in supporting the HMNS, most of these papers show the angular velocity profile of the merged object before the eventual collapse to a black hole. The typical profile extracted from simulations characteristically shows a plateau near the rotation axis and a certain distance from the axis shows a nearly power law behavior. The power index seems to differ from simulation to simulation, but generally does not agree with the so-called “j-const. law” (Eriguchi & Müller 1985) of rotation, which has been so far the only choice available to construct equilibrium models of differentially rotating stars.

Models of rapidly rotating stars in general relativity have been studied since the 70s, when large numerical computing facilities became available. The centrifugal deformation and general relativistic gravity make these investigations fully reliant on numerical methods. Since the pioneering work of Butterworth & Ipser (1976), these studies have included progressively more sophisticated aspects, such as nuclear matter

\* filippo.galeazzi@aei.mpg.de

EOS, degrees of differential rotation, magnetic fields and quite recently meridional flows (Birkel et al. 2010). We here name the following references of such studies: Butterworth & Ipsier (1976) ; Komatsu et al. (1989) ; Bonazzola et al. (1993) ; Stergioulas & Friedman (1995) ; Baumgarte et al. (2000) ; Ansorg et al. (2002). For more comprehensive collection of literatures, see Stergioulas (2003).

However, it is surprising to note that all of these studies have used just a single kind of ansatz on the rotational angular velocity profile (namely the “j-const. law”, which include uniformly-rotating stars as a limiting case (Section 2.2)).

In this work we introduce a new parametrized functional form of the rotation profile that enables us to investigate a broader class of differentially rotating stars. In particular, our new rotation law reproduces different power laws in the outer envelope of the angular velocity distribution (see Section 2.2) with which it is possible to match the profile of the HMNS. To analyze the impact of the law of rotation on the maximum allowed mass for the differentially-rotating neutron star we construct equilibrium sequences by imposing a fixed value of  $T/|W|$  close to what is the classical limit for the onset of the *secular* instability; rotating neutron stars are known to be destabilized by the effect of dissipative mechanisms like viscosity and gravitational radiation reaction (Chandrasekhar-Friedman-Schutz (CFS) instability; Chandrasekhar (1970); Friedman & Schutz (1978)). We show that the classical secular instability criterion is satisfied only for a limited class of the rotation profiles.

The paper is organized as follows. In Section 2 we briefly review the formalism of the equations and the numerical method used to solve them. Then we describe the new functional form of the rotation profile. In Section 3 we construct equilibrium sequences of rotating stars using the new rotation profile. Discussions are given in the final section.

## 2. Formulation

### 2.1. Equations for fluid and spacetime

We construct configurations for an *axisymmetric* and *stationary* rotating perfect fluid in general relativity. The spacetime is assumed to be asymptotically flat and the flow is assumed to be circular (the velocity is only in the azimuthal direction). In this case we have two Killing vectors (Bardeen 1970) and can choose a coordinate system in such a way that the metric of the spacetime is written as (e.g., Komatsu et al. (1989)),

$$ds^2 = -e^{2\nu} dt^2 + e^{2\alpha} (dr^2 + r^2 d\theta^2) + e^{2\beta} r^2 \sin^2 \theta (d\varphi - \omega dt)^2, \quad (1)$$

where the spherical polar coordinates  $(r, \theta, \phi)$  are used. The metric potentials  $\alpha, \beta, \nu$  and  $\omega$  are functions of  $r$  and  $\theta$  only.<sup>1</sup> The energy momentum tensor  $T^{ab}$  of a perfect fluid is

$$T^{ab} = (\epsilon + p)u^a u^b + pg^{ab} \quad (2)$$

where  $\epsilon$ ,  $p$  and  $u^a$  are the total energy density, the pressure and the four velocity, respectively.

The basic equations are: 1) Einstein’s equation for the metric potentials  $G_{ab} = 8\pi T_{ab}$ , 2) rest mass conservation  $\nabla_a(\rho u^a) = 0$ , which is trivially satisfied under the present assumptions and 3) stress-energy conservation  $\nabla_b T^{ab} = 0$ .

As described in Komatsu et al. (1989), the components of Einstein’s equation are cast into 4 equations for the potentials, three of which are elliptic partial differential equations. They are

transformed into convenient integral equations by using appropriate Green’s functions.

The spatial linear velocity  $V$  of the flow with respect to an observer with zero angular momentum is given by

$$V = e^{\beta-\nu} r \sin \theta (\Omega - \omega) \quad (3)$$

where  $\Omega = u^\varphi/u^t$  is the angular frequency of the fluid measured in the asymptotic inertial frame. We next introduce the specific angular momentum<sup>2</sup>  $j$ :

$$j = -\frac{u_\varphi}{u_t}. \quad (4)$$

Using these quantities, we can write the equilibrium equations for a stationary configuration as

$$\frac{\partial_A p}{\epsilon + p} + \partial_A \nu - \frac{1}{1 - V^2} V \partial_A V + \frac{j}{1 - j\Omega} \partial_A \Omega = 0 \quad (A = r, \theta). \quad (5)$$

Assuming the fluid to be barotropic, the condition of integrability for Eq.(5), can be written as

$$\frac{j}{1 - j\Omega} = g(\Omega), \quad (6)$$

by introducing an arbitrary functional  $g$ , which is detailed in the next subsection. The first integral of motion for a stationary solution can be written as

$$\int \frac{dp}{\epsilon + p} + \nu + \frac{1}{2} \ln(1 - V^2) + \int g(\Omega) d\Omega = 0. \quad (7)$$

The components of Einstein’s equation and the first integral of hydrostatic equation can be iteratively solved as described in Komatsu et al. (1989)

### 2.2. Rotation profile

To exploit the first integral of the hydrostatic equation, we need to impose the integrability condition for Eq.(6). Different choices of functional form  $g(\Omega)$  would lead to various classes of differential-rotation profiles. All previous studies of differentially-rotating relativistic stellar models assume the simplest linear functional form,

$$g(\Omega) = A^2(\Omega_c - \Omega), \quad (8)$$

where  $A$  is a constant with the dimensions of a length and  $\Omega_c$  is the angular velocity on the axis of rotation.

This choice is termed as “j-const. law” since the Newtonian limit of the specific angular momentum  $j$  is that of “j-const. law” in Newtonian rotating stars (Eriguchi & Müller 1985).

We here introduce a more flexible form of the rotation profile as

$$g(\Omega) = \frac{\frac{R_0^2}{\Omega_c^2} \Omega (\Omega^\alpha - \Omega_c^\alpha)}{1 - \frac{R_0^2}{\Omega_c^2} \Omega^2 (\Omega^\alpha - \Omega_c^\alpha)}, \quad (9)$$

where  $\alpha$ ,  $R_0$  and  $\Omega_c$  are constants. The corresponding specific angular momentum is

$$j = \frac{R_0^2}{\Omega_c^2} \Omega (\Omega^\alpha - \Omega_c^\alpha). \quad (10)$$

<sup>2</sup> This quantity is one definition of specific angular momentum in general relativity. For different definitions, see Kozłowski et al. (1978).

<sup>1</sup> We use geometrized units,  $c = G = 1$ .

$\alpha$	-1	-4/3	-2	-4
$\Omega_{outer}$	$R^{-2}$	$R^{-3/2}$	$R^{-1}$	$R^{-1/2}$
power law in envelope	j-const.	Keplerian	v-const.	HMNS

**Table 1.** Choosing different  $\alpha$ , it is possible to introduce different power law distributions of the angular velocity in the outer region of a star. We here tabulate the Newtonian limits of particular choices of  $\alpha$ . “j-const.” refers to constant specific angular momentum. “v-const.” is for constant linear velocity. “HMNS” is the approximate power law of some of numerical relativistic simulations with HMNS formation (e.g., Shibata & Uryū (2002); Baiotti et al. (2008)).

The physical significance of the parameters  $\alpha$ ,  $R_0$  and  $\Omega_c$  in the profile is easily seen if we consider its Newtonian limit. Then the angular frequency is written as

$$\Omega = \Omega_c \left( 1 + \left( \frac{R}{R_0} \right)^2 \right)^{\frac{1}{\alpha}} \quad (11)$$

where  $R = r \sin \theta$ . For  $R \ll R_0$ , we have  $\Omega \sim \Omega_c$ , while for  $R \gg R_0$ ,

$$\Omega \sim \Omega_c \left( \frac{R}{R_0} \right)^{\frac{2}{\alpha}}. \quad (12)$$

This means that the rotation profile has an inner plateau inside  $R \sim R_0$  and a power law envelope for  $R \gg R_0$ . The introduction of the index  $\alpha$  is an important feature of the new profile: as shown in Table 1, it is possible to reproduce different rotation laws by choosing different values for  $\alpha$ .

For some interesting cases ( $\alpha \in \{-1, -2, -4\}$ ), it is possible to integrate analytically the expression for  $g(\Omega)$  (see Appendix). It is important to note that for  $\alpha = -1$  the  $j$ -constant type of law is recovered – the two functional forms must agree in the limit of weak gravity. This particular case is marginally stable under Rayleigh’s local stability criterion of axisymmetric instability, which states that the specific angular momentum must not decrease outward in a stable star. Values of  $\alpha$  smaller than  $-1$  satisfy this condition (and hence are stable).  $\alpha > 0$  also satisfies this condition, but a star cannot be spun up rapidly enough to allow the appearance of the CFS instability, because it easily reaches its mass-shedding limit.

We now apply the new rotation law to construct equilibrium configurations of differentially rotating neutron stars and study their dependence on  $\alpha$ . Each configuration is defined by five parameters: the axis ratio  $r_p/r_e$ , the polytropic index  $N$ , the maximum density  $\rho_{max}$  and the two parameters of the rotation law,  $R_0$  and  $\alpha$ .

## 3. Results

### 3.1. Numerical code

We construct sequences of axisymmetric and differentially rotating objects using the code discussed in Komatsu et al. (1989). The code iteratively solves Einstein’s equation and the first integral of motion for a stationary fluid configuration.

For all computation we used a grid with 600 points in the  $r$ -direction and 300 in the  $\theta$ -direction. The radial grid is set up in such a way that the inner uniformly-distributed 300 grid points just cover the whole star (on the equator the 300th point from the origin always corresponds to the surface of the star). Outside

the star we adopt the “compactified” coordinate as in Cook et al. (1992), to take into account the exact boundary condition at the radial infinity.

For a given EOS, a functional of the rotation profile and maximum density, the code requires information on “how rapidly” the star is rotating. To this end, it is more convenient to specify a parameter that measures the deformation induced by the rotation rather than the angular momentum or the rotational frequency. We follow Komatsu et al. (1989) in fixing the ratio of the polar coordinate radius of the star to the equatorial radius. The physical parameters of rotation as well as other physical quantities are then computed.

### 3.2. Equation of state

In the current study we use a polytropic equation of state, with the index  $N = 1$  to model neutron stars,

$$p = \kappa \rho^{1+1/N}, \quad \epsilon = \rho + Np. \quad (13)$$

Typical neutron star masses and radii are recovered when we set  $\kappa = 100$  in geometrized units. We fix this parameter for all the sequences to have a crude model of the nuclear equation of state for neutron matter. In a subsequent paper we will investigate the dependence of the space of configurations on the EOS, using realistic cold and finite-temperature EOSs.

### 3.3. Parameters

To obtain an equilibrium model, we fix the parameters of the rotation profile,  $\alpha$  and  $R_0$ , then choose the maximum density  $\rho_{max}$  and the coordinate axis ratio. In our code this set of parameters uniquely determines an equilibrium configuration, whose physical characteristics such as mass, compactness and angular momentum, angular frequency at the centre are computed once the solution is obtained. Rest mass and gravitational mass are computed by using the standard formula (see e.g. Bardeen (1970)). An important measure of rotation, the  $T/|W|$  parameter, is introduced as in Komatsu et al. (1989). This is used both in Newtonian and general relativistic studies of rotating stars and defined as the ratio of rotational kinetic energy to gravitational binding energy (see Komatsu et al. (1989) for details). It characterises the overall strength of rotation of the star. Classical studies suggest that when  $T/|W| \sim 0.14$ , bar-shaped equilibria bifurcate (into “Jacobi” or “Dedekind” type equilibrium sequences) and  $T/|W| \sim 0.27$  marks the onset of dynamical instability of axisymmetric configurations (Tassoul 1978). In general relativity numerical simulations point to a rather lower limit,  $T/|W| \sim 0.25$  (Manca et al. 2007).

### 3.4. Numerical equilibrium sequences

For a given rotation profile and a maximum density, we start from a non-rotating model (the polar-to-equatorial axis ratio is equal to unity), and decrease the ratio to obtain stars with increasingly rapid rotation. We terminate the sequence if one of the following conditions is satisfied: 1)  $T/|W| = 0.14$ . This is the classical criterion at which CFS instability or viscous instability sets in for a bar-shaped deformation (the actual critical point depends weakly on both the equation of state and degree of differential rotation (Karino & Eriguchi 2002)). 2) Mass-shedding limit. The last condition is reached when the angular frequency of matter at the equatorial surface comes close to local Keplerian frequency and a further spin-up of a star leads to shedding of

mass. Beyond this point it is not possible to construct equilibrium configurations. 3) Topology change. When the degree of differential rotation is large the maximum density may move away from the rotation axis. When the value of the axis ratio reaches zero, the star develops a hole on the rotation axis. The equilibrium sequence may be continued beyond this point, but we are not interested in this toroidal shape configuration as a model of a neutron star.

Concerning the last point above, we should note that the structure of the parameter space is quite complex, as has been analyzed by Ansorg et al. (2009). The toroidal and the spheroidal configurations form disjoint families of solutions separated by a mass shedding region. Increasing the degree of differential rotation by reducing the value of the  $R_0$  parameter, the two families join again in the parameter space. The area of the region separating the two topologically different families depends on the  $\rho_{max}$  of the configuration, becoming smaller as the latter is increasing. Stated differently, starting from the Newtonian limit and going to the more general relativistic case, it becomes more and more complicated to find a value of  $R_0$  for which the solution can reach the toroidal family, in fact the separation increases between the two types of solutions. We have studied the parameter space of the solutions for the three different rotation laws analyzed here, and will collect the results along with the dependency hidden in the EOS in the followup paper.

### 3.5. Stellar mass in parameter space

To visualize our results, we plot gravitational mass of stellar models in the parameter space. Figure 1 shows the surfaces of equilibrium models embedded in the  $R_0 - \rho_{max} - M/M_{sun}$  space, where  $M$  is the gravitational mass in units of solar masses, for three different values of the parameter  $\alpha$ :  $\alpha = -1$  (top panel),  $\alpha = -2$  (middle panel) and  $\alpha = -4$  (bottom panel). In order to have the same degree of differential rotation for all the models with a constant  $R_0$ , following the prescription of Baumgarte et al. (2000), we define:

$$\hat{R}_0 = R_0/R_c, \quad (14)$$

where  $R_c$  is the circumferential radius.

On the bases of these plots, we marked each parameter pair ( $\rho_{max}, \hat{R}_0$ ) with different symbols to indicate how the equilibrium sequence ends. The triangles correspond to the parameters for which  $T/|W|$  of the model reaches 0.14 (and the computations are stopped there). The dots correspond to the parameter pairs for which the sequence terminates at the mass-shedding limit. The solid lines are for the parameters for which the sequence of spheroids ends with a topological change.

As mentioned in Section 3.4, our sequences terminate at the three different criteria. Therefore one needs to be careful in reading these figures. It is important to stress that for the sequences terminating at  $T/|W| = 0.14$  and at the topological change, the value of mass plotted here is *not* the maximum mass of the sequence. The solutions of the toroidal class do not possess a value for the maximum mass, instead this quantity can arbitrarily increase as the torus becomes thinner and thinner along the sequence of equilibrium figures (see. Ansorg et al. (2003)).

It is seen from Eq.(9) that the angular velocity profile becomes uniform as  $\hat{R}_0 \rightarrow \infty$ . In this rigid rotation limit, the sequence of  $N = 1$  polytropes is known to terminate with mass-shedding state before reaching  $T/|W| = 0.14$ . The degree of differential rotation depends both on the power-law exponent  $\alpha$  and on the radius  $R_0$ . We may regard it as *weak* when the profile is close to uniform rotation (i.e.  $R_0 \rightarrow \infty$  and/or  $\alpha \rightarrow -\infty$ ).

As in the case of uniform rotation, for stars with weak differential rotation the centrifugal force at the equator on the surface reaches a value at which the star sheds mass before its  $T/|W|$  value reaches 0.14. In this case all the sequences terminate at mass-shedding limit before reaching  $T/|W| = 0.14$  or the point of topology change. However a star with sufficiently strong differential rotation can store large rotational energy deep inside the star and allow the surface angular frequency to be smaller than that of the mass-shedding limit. Therefore a star with  $\alpha = -1$  or  $-2$  reaches the critical point  $T/|W| = 0.14$  before encountering mass-shedding or topology change, provided that  $\hat{R}_0$  is small enough (that is a smaller core region of nearly uniform rotation). For these choices of  $\alpha$  and sufficiently small  $\hat{R}_0$ , we also see the appearance of topological change *before* the critical  $T/|W| = 0.14$  is reached (represented as the triangles in Fig.1). Indeed, the sequences which we terminate at  $T/|W| = 0.14$  will eventually see the topology change if extended to faster rotation.

An important observation here is that for  $\alpha = -4$  none of the models reach  $T/|W| = 0.14$  before mass shedding occurs, and for  $\alpha = -1$ , and  $-2$  we need to set  $\hat{R}_0$  sufficiently small (i.e., enabling high degree of differential rotation) to have the critical  $T/|W|$  before topology change or mass shedding occurs.

## 4. Summary and Discussion

We have introduced a new rotation profile to study equilibrium sequences of differentially rotating relativistic stars. Compared with the previous studies, which assume only one type of rotation profile, we are now able to investigate a broader class of rotating stars.

As a first step towards systematic studies, we focus on the simplest neutron star model with a polytropic EOS with index  $N = 1$ . For the rotation profiles that allow analytic expressions in the Eq. (5), we computed sequences of spheroidal equilibria that start from non-rotating stars. Special attention is paid to the appearance of the critical point to the secular instability (CFS or viscous instability) to bar-shaped deformation of the star. We see that the appearance of the critical point may occur for rather strong differential rotation in the case of  $\alpha = -1$  and  $-2$  in Eq.(9), which corresponds respectively to so-called “j-const.” and “v-const.” rotation profiles in Newtonian stars (Eriguchi & Müller 1985). Even in these cases, the critical point does not appear before the configuration changes from a spheroidal topology to a toroidal one, unless the parameter  $R_0$  in Eq.(9) is sufficiently small.

When  $\alpha = -4$  instead there seems no critical point of CFS instability before the equilibrium sequences reach their mass-shedding limit. This last case is relevant since it appears to mimic the approximate rotation profile of some of the quasi-stationary HMNSs seen in the numerical simulations of neutron star mergers. However these stars may be susceptible to the relatively new class of dynamical instability (so-called “low  $T/|W|$  instability”, e.g. Centrella et al. (2001); Shibata et al. (2002); Watts et al. (2003); Saijo & Yoshida (2006); Ou & Tohline (2006); Baiotti et al. (2008)), whose existence relies on the strong shear flow (Watts et al. (2005); Corvino et al. (2010)). Indeed, numerical simulations of binary NSs do indicate that the HMNS develops a bar deformation (e.g. Shibata & Uryū (2002); Baiotti et al. (2008)) on top of the background star with approximate axisymmetry. It would be interesting to study the appearance of low  $T/|W|$  instability by using our equilibrium stars with different rotation profiles since the survival time of the merger remnant could be an important diagnostic. The observation of the delay between detection of the gravitational wave signal

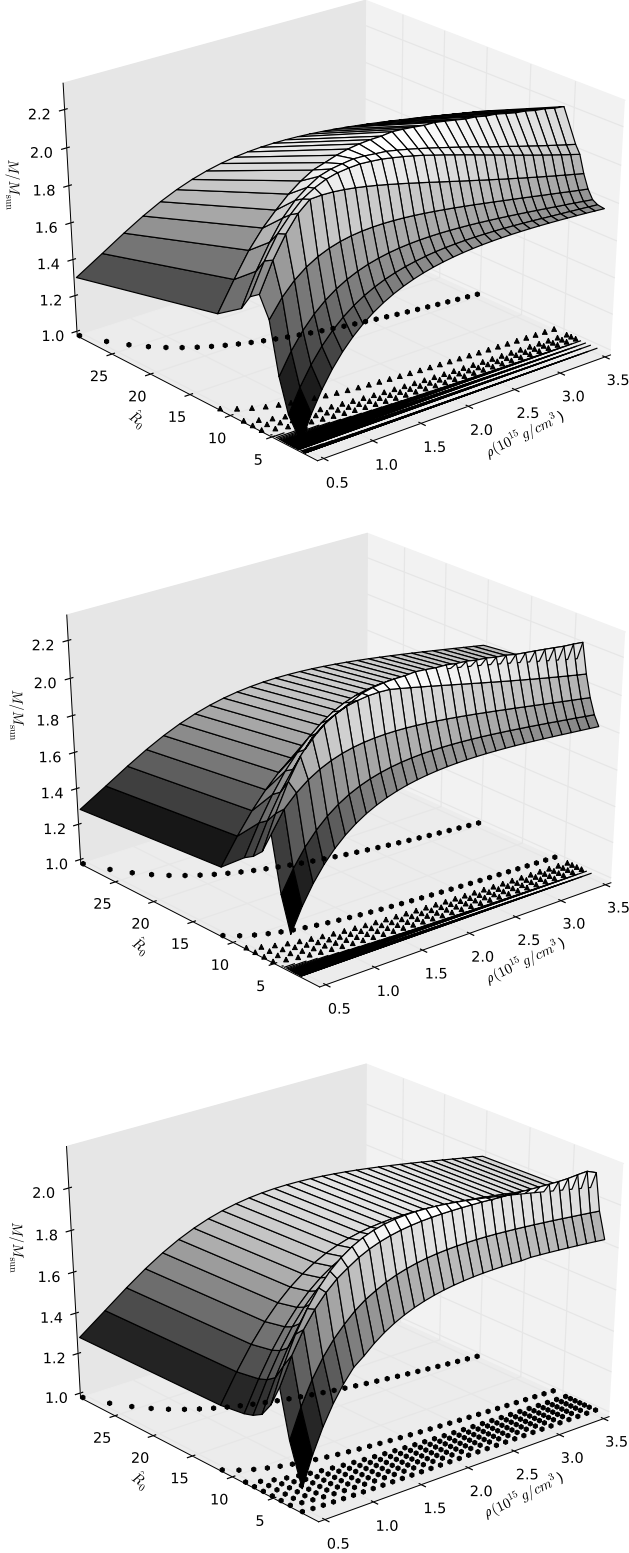


**Fig. 1.** Two-dimensional surfaces of equilibrium models of differentially rotating neutron stars embedded in the space  $\hat{R}_0 - \rho_{max} - M/M_{sun}$ . The first panel is for  $\alpha = -1$ , the second one is for  $\alpha = -2$  and the last one is for  $\alpha = -4$ . The lines at the bottom of each panel are drawn to clarify which of the three terminal conditions (see Section 3.4) of sequence applies. Triangles are for sequences reaching  $T/|W| = 0.14$ , dots are for sequences terminating with mass shedding and thick solid lines are for the case when topology change occurs.

form a binary neutron stars merger and the possible observation of the short gamma ray burst counterpart would then help to put constraints on the internal structure of a NS.

*Acknowledgements.* We thank Marcus Ansorg and Carlos Palenzuela for useful discussions. This work is supported in part by a Grant-in-Aid for Scientific Research (C) of Japan Society for the Promotion of Science (20540225). FG wants to thank Aaryn Tonita for the essential support in this work, Sam Lander for the fruitful discussions and finally Luciano Rezzolla for the continuous support that he devoted in this project.

## Appendix A: Integration of $g(\Omega)$

For some interesting cases, we have an analytic expression for the integral of  $g(\Omega)$  which appears in Eq.(7).

We define a parameter  $k := (R_0\Omega_c)^2$  and normalize  $\Omega$  as  $\xi := \Omega/\Omega_c$ . Then the integration of the functional  $g(\Omega)$  is written as

$$\int g(\Omega)d\Omega = \int \frac{k\xi(\xi^\alpha - 1)}{1 - k\xi^2(\xi^\alpha - 1)}d\xi. \quad (\text{A.1})$$

For  $\alpha = -1$ , the right hand side reduces to

$$\sqrt{\frac{k}{4-k}} \text{Arctan}\left(\sqrt{\frac{k}{4-k}}(2\xi - 1)\right) - \frac{1}{2} \ln(1 + k\xi(\xi - 1)). \quad (\text{A.2})$$

For  $\alpha = -2$ , it reduces to

$$\frac{\ln(1 + k(\xi^2 - 1)) - 2k \ln \xi}{2(k - 1)}. \quad (\text{A.3})$$

Finally, for  $\alpha = -4$  we have

$$-\ln \xi + \frac{1}{2\sqrt{1+4k^2}} \cdot \ln\left(\frac{-1 + \sqrt{1+4k^2} - 2k\xi^2}{+1 + \sqrt{1+4k^2} + 2k\xi^2}\right). \quad (\text{A.4})$$

## References

- Anderson, M., Hirschmann, E. W., Lehner, L., et al. 2008, Physical Review Letters, 100, 191101
- Ansorg, M., Gondek-Rosińska, D., & Villain, L. 2009, MNRAS, 396, 2359
- Ansorg, M., Kleinwächter, A., & Meinel, R. 2002, Astron. Astrophys., 381, L49
- Ansorg, M., Kleinwächter, A., & Meinel, R. 2003, ApJ, 582, L87
- Baiotti, L., Giacomazzo, B., & Rezzolla, L. 2008, Phys. Rev. D, 78, 084033
- Balbus, S. A. & Hawley, J. F. 1991, ApJ, 376, 214
- Bardeen, J. M. 1970, ApJ, 162, 71
- Baumgarte, T. W., Shapiro, S. L., & Shibata, M. 2000, ApJ, 528, L29
- Baym, G., Pethick, C., & Pines, D. 1969, Nature, 224, 872
- Birkel, R., Stergioulas, N., & Müller, E. 2010, ArXiv e-prints
- Bonazzola, S., Gourgoulhon, E., Salgado, M., & Marck, J. A. 1993, A&A, 278, 421
- Butterworth, E. M. & Ipser, J. R. 1976, ApJ, 204, 200
- Centrella, J. M., New, K. C. B., Lowe, L. L., & Brown, J. D. 2001, ApJ, 550, L193
- Chandrasekhar, S. 1970, Physical Review Letters, 24, 611
- Cook, G. B., Shapiro, S. L., & Teukolsky, S. A. 1992, ApJ, 398, 203
- Corvino, G., Rezzolla, L., Bernuzzi, S., De Pietri, R., & Giacomazzo, B. 2010, Classical and Quantum Gravity, 27, 114104
- Cutler, C. & Lindblom, L. 1987, ApJ, 314, 234
- Dimmelmeier, H., Font, J. A., & Müller, E. 2002, A&A, 393, 523
- Duez, M. D., Liu, Y. T., Shapiro, S. L., Shibata, M., & Stephens, B. C. 2006, Phys. Rev. D, 73, 104015
- Eriguchi, Y. & Müller, E. 1985, A&A, 146, 260
- Friedman, J. L. & Schutz, B. F. 1978, ApJ, 222, 281
- Giacomazzo, B., Rezzolla, L., & Baiotti, L. 2010, ArXiv e-prints
- Karino, S. & Eriguchi, Y. 2002, ApJ, 578, 413
- Komatsu, H., Eriguchi, Y., & Hachisu, I. 1989, MNRAS, 237, 355
- Kozłowski, M., Jaroszynski, M., & Abramowicz, M. A. 1978, A&A, 63, 209
- Manca, G. M., Baiotti, L., DePietri, R., & Rezzolla, L. 2007, Classical and Quantum Gravity, 24, 171
- Ott, C. D., Burrows, A., Livne, E., & Walder, R. 2004, ApJ, 600, 834

- Ott, C. D., Dimmelmeier, H., Marek, A., et al. 2007, *Physical Review Letters*, 98, 261101
- Ou, S. & Tohline, J. E. 2006, *ApJ*, 651, 1068
- Pines, D. & Alpar, M. A. 1985, *Nature*, 316, 27
- Ruffert, M. & Janka, H. 2001, *A&A*, 380, 544
- Ruffert, M., Janka, H., & Schaefer, G. 1996, *A&A*, 311, 532
- Saijo, M. & Yoshida, S. 2006, *MNRAS*, 368, 1429
- Sawyer, R. F. 1989, *Phys. Rev. D*, 39, 3804
- Shibata, M., Karino, S., & Eriguchi, Y. 2002, *MNRAS*, 334, L27
- Shibata, M. & Taniguchi, K. 2006, *Phys. Rev. D*, 73, 064027
- Shibata, M. & Uryū, K. 2002, *Progress of Theoretical Physics*, 107, 265
- Spruit, H. C. 1999, *A&A*, 349, 189
- Stergioulas, N. 2003, *Living Reviews in Relativity*, 6, 3
- Stergioulas, N. & Friedman, J. 1995, *Astrophys. J.*, 444, 306
- Takiwaki, T. & Kotake, K. 2010, *ArXiv e-prints*
- Tassoul, J. 1978, *Theory of rotating stars*, Princeton Series in Astrophysics, Princeton: University Press
- Watts, A. L., Andersson, N., Beyer, H., & Schutz, B. F. 2003, *MNRAS*, 342, 1156
- Watts, A. L., Andersson, N., & Jones, D. I. 2005, *ApJ*, 618, L37